JOURNAL OF NATURAL PRODUCTS

Article

pubs.acs.org/jnp

Absolute Configuration and Conformational Analysis of Brevipolides, Bioactive 5,6-Dihydro-α-pyrones from *Hyptis brevipes*

G. Alejandra Suárez-Ortiz,[†] Carlos M. Cerda-García-Rojas,[‡] Adriana Hernández-Rojas,[†] and Rogelio Pereda-Miranda*[,†]

[†]Departamento de Farmacia, Facultad de Química, Universidad Nacional Autónoma de México, Circuito Exterior Ciudad Universitaria, México City, D. F. 04510 México

[‡]Departamento de Química y Programa de Posgrado en Farmacología, Centro de Investigación y de Estudios Avanzados del Instituto Politécnico Nacional, A.P. 14-470, México City, D. F. 07000 México

Supporting Information

ABSTRACT: The (6′*S*)-configuration of brevipolides A–J (**1**–**10**), isolated from *Hyptis brevipes*, was established by X-ray diffraction analysis of **9** in conjunction with Mosher's ester analysis of the tetrahydro derivative **11** obtained from both geometric isomers **8** and **9** as well as by chemical correlations. The structure of the new brevipolide J (**10**) was characterized through NMR and MS data as having the same 6-heptyl-5,6-dihydro-2*H*-pyran-2-one framework possessing the cyclopropane moiety of all brevipolides but substituted by an isoferuloyl group instead of the *p*-methoxycinnamoyl moiety found in **8** and **9**. Conformational analysis of these cytotoxic 6-heptyl-5,6-dihydro-α-pyrones was carried out on compound **9** by application of a protocol based on comparison between experimental and DFT-calculated vicinal $^{1}H-^{1}H$ NMR coupling constants. Molecular modeling was used to correlate minimum energy conformers and observed electronic circular dichroism transitions for the isomeric series of brevipolides. Compounds **7**–**10** exhibited moderate activity (ED_{50} 0.3–8.0 μg/mL) against a variety of tumor cell lines.

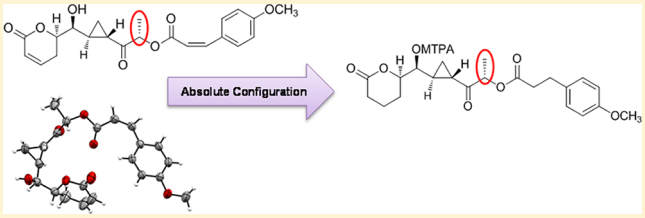

α,β-Unsaturated δ-lactones, well-known Michael acceptors, constitute the pharmacophoric group of a broad range of natural products.[1] Many of these compounds display pharmacologically relevant properties, e.g., antimicrobial, cytotoxic, and antitumoral activities.[2,3] These bioactive products, occurring in several members of the mint family (Lamiaceae)[4−6] (Figure S1, Supporting Information), comprise polyacylated-6-heptyl-5,6-dihydro-2*H*-pyran-2-ones particularly abundant in the genus *Hyptis*.[3,7,8] They are structurally related to pironetin (Figure S2, Supporting Information), an anticancer acetogenin of microbial origin that selectively targets Lys-352 of α-tubulin.[9]

Recently, six cytotoxic compounds, brevipolides A–F (**1**–**6**, Figure 1), all of which share a 6-heptyl-5,6-dihydro-2*H*-pyran-2-one framework bearing a cyclopropane moiety, were isolated from *Hyptis brevipes* collected in Indonesia.[10] These products were structurally related to the skeletal class first characterized in compound **7** and related compounds **8** and **9** from *Lippia alva* (Verbenaceae), which were identified as inhibitors of the chemokine receptor CCR5 (the principal human immunodeficiency virus type 1 co-receptor).[11] Compound **7** was also found to be active in an enzyme-based ELISA NF-κB assay.[10] However, the absolute configuration at C-6′ was not established for any of these 6-heptyl-5,6-dihydro-2*H*-pyran-2-ones. This situation prompted us to undertake a study directed to the assignment of the absolute configuration and conformational analysis of compound **9**, as a representative model for all related brevipolides, in order to obtain an accurate description of their three-dimensional properties by applying a protocol

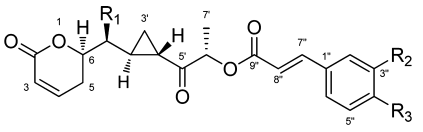

1	R_1 = OAc	R_2 = H	R_3 = OH
2	R_1 = OH	R_2 = OH	R_3 = OH
3	R_1 = OAc	R_2 = OH	R_3 = OH
7	R_1 = OH	R_2 = H	R_3 = OH
8	R_1 = OH	R_2 = H	R_3 = OMe
10	R_1 = OH	R_2 = OH	R_3 = OMe

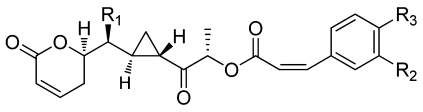

4	R_1 = OAc	R_2 = H	R_3 = OH
5	R_1 = OH	R_2 = OH	R_3 = OH
6	R_1 = OAc	R_2 = H	R_3 = OH
9	R_1 = OH	R_2 = H	R_3 = OMe

Figure 1. Brevipolides from *Hyptis brevipes*.

Received: October 26, 2012
Published: January 2, 2013

based on the systematic comparison between DFT theoretical and experimental vicinal ^{1}H NMR coupling constants.[12,13]

In the present investigation, compounds **7**–**9** and the new natural product **10** were isolated from a Mexican collection of *H. brevipes* and given the trivial names of brevipolides G–J, respectively. A combination of X-ray diffraction analysis, chiroptical measurements, chemical correlations, and Mosher ester derivatization was used to confirm the absolute configuration of these compounds.

RESULTS AND DISCUSSION

Aerial parts of *H. brevipes* were powdered and extracted with $CHCl_3$. The extract was fractionated by column chromatography on silica. The fractions containing 5,6-dihydro-2*H*-pyran-2-ones were purified by preparative reversed-phase HPLC through application of the recycling technique.[14] This procedure afforded **7**–**10**, which displayed moderate cytotoxicity against nasopharyngeal cancer cells (KB) with IC_{50} values of 0.3–2.0 μg/mL (Table S7, Supporting Information).

Compound **7** showed a quasi-molecular ion at m/z 387.1455 $[M + H]^+$ by HRFABMS in the positive mode, consistent with the molecular formula $C_{21}H_{24}O_7$. The molecular formula of compound **8** was established as $C_{22}H_{25}O_7$ by HRFABMS with a quasi-molecular ion peak $[M + H]^+$ at m/z 401.1595. Compound **9** showed the same ion, thus indicating that **8** and **9** are structural isomers. Methylation of the phenolic group of **7** with diazomethane afforded a product that was identical to compound **8**. ^{1}H and ^{13}C NMR chemical shifts for **7**–**9** are listed in Table S1 (Supporting Information). All values were identical to those reported for the compounds isolated from *Lippia alva*.[11]

The molecular formula of the new natural product **10** was established as $C_{22}H_{24}O_8$ by HRFABMS, showing a quasi-molecular $[M + H]^+$ ion peak at m/z 416.1467. Compound **10** exhibited the characteristic ^{1}H and ^{13}C NMR signals (Table 1; Figures S9 and S10, Supporting Information) for the 6-heptyl-5,6-dihydro-2*H*-pyran-2-one framework. The α,β-unsaturated δ-lactone system was identified through the characteristic resonance for the C-2 carbonyl group (δ 164.0) and the C-3 and C-4 vinylic protons at δ 6.02 and 6.98, respectively, as part of an AMX_2 spin-system with the C-5 methylene group (δ 23.4), which is also coupled to H_6 resonating at δ 4.52. The coupling constants between the methylene protons at C-5 and H_6 ($J_{5ax\text{-}6}$ = 12.3; $J_{5eq\text{-}6}$ = 3.8) indicated the pseudoequatorial orientation of the side chain.[4,7] The heptyl side chain was identified through the C-7′ terminal methyl group (δ 1.60) as part of an AX_3 spin-system with the downshifted methine signal at C-6′ (δ 5.30), corroborating the substitution of this stereogenic center by an ester group. The observed $^3J_{CH}$ correlation of the terminal methyl group with the carbonyl carbon at δ 206.7 permitted placement of the carbonyl group at C-5′. The multiplicities of the signals in the upfield region at δ 2.28 (H-4′), 1.60 (H-2′), 1.34 (H-3′$_{proS}$), and 1.12 (H-3′$_{proR}$) were attributed to the presence of a cyclopropane ring. $^{2,3}J_{CH}$ correlations from H-6 to H-1′ (δ 3.70) and H-2′ indicated that the lactone and cyclopropane moieties were connected through a secondary hydroxy group at C-1′ (δ 71.8). The characteristic signals for an isoferuloyl group, as the C-6′ substituent, were also observed (Table 1).

X-ray diffraction analysis was undertaken to establish the relative configuration of **9** (Figure 2). The crystal parameters and X-ray coordinates are included in Tables S2–S6 (Supporting Information). Because of the bent U-shaped

Table 1. ^{1}H and ^{13}C NMR Chemical Shifts and Coupling Constants for 10[a]

position	δ_H (J in Hz)	δ_C
2		164.0
3	6.02 ddd (9.7, 2.2, 0.9)	120.8
4	6.98 ddd (9.7, 6.4, 2.2)	146.1
5_{ax}	2.70 dddd (18.5, 12.3, 2.2, 2.2)	23.4
5_{eq}	2.52 dddd (18.5, 6.4, 3.8, 0.9)	
6	4.52 ddd (12.3, 3.8, 3.8)	80.7
1′	3.70 dd (6.3, 3.8)	71.8
2′	1.60 dddd (8.9, 6.3, 6.3, 3.4)	26.6
$3'_{proR}$	1.12 ddd (8.9, 6.3, 4.0)	14.5
$3'_{proS}$	1.34 ddd (8.5, 4.0, 3.9)	
4′	2.28 ddd (8.5, 3.9, 3.4)	21.5
5′		206.7
6′	5.30 q (7.0)	75.2
7′	1.60 d (7.0)	16.1
1″		127.7
2″	7.13 d (1.9)	113.2
3″		145.9
4″		148.9
5″	6.84 d (8.3)	110.6
6″	7.03 dd (8.3, 1.9)	122.1
7″	7.64 d (15.9)	146.1
8″	6.34 d (15.9)	114.9
9″		166.7
OMe	3.92 s	56.0

[a]NMR spectra were acquired in $CDCl_3$ at 25 °C. Chemical shifts (δ) are in ppm relative to TMS. The spin coupling (J) is given in parentheses (Hz) and was obtained by nonlinear fit of the experimental ^{1}H NMR spectrum to the simulated spectrum generated by iteration of spectral parameters (^{1}H chemical shifts, J-couplings, and line width).

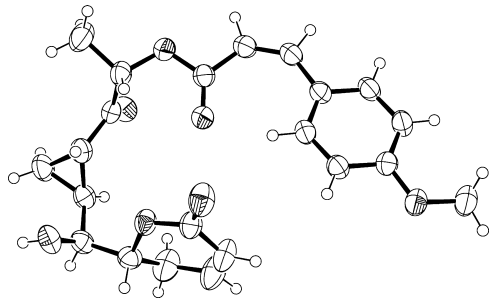

Figure 2. X-ray ORTEP drawing of brevipolide I (**9**).

geometry adopted by this brevipolide, intermolecular hydrogen bonds (2.06 Å) between the oxygen of the lactone group and the hydroxy moiety at C-1′ were observed in the crystal packing (Figure S24, Supporting Information). To ascertain the absolute configuration of compounds **8** and **9**, catalytic hydrogenation using Pd/C was carried out to reduced both double bonds, yielding a convergent tetrahydro derivative (**11**), followed by application of the Mosher's ester protocol[15] involving its free C-1′ hydroxy group. The hydrogenation product derived from either **8** or **9** displayed identical physical data and ^{1}H and ^{13}C NMR spectra (Figures S16 and S17, Supporting Information), enabling us to assume that the absolute configurations for all stereogenic centers of both compounds were the same. The tetrahydro derivative **12** was similarly prepared from **10**. The chemical shift difference values (Table 2) obtained by comparing the relevant ^{1}H NMR data of

dx.doi.org/10.1021/np300740h | J. Nat. Prod. 2013, 76, 72–78

Table 2. ^{1}H NMR Chemical Shift Data for Diagnostic Signals from the (*S*)- and (*R*)-Ester Derivatives of Hydrogenated Derivative 11

					proton chemical shifts ($\Delta\delta_H = \delta_S - \delta_R$)[a]								
MTPA-ester	H-5ax	$\Delta\delta_H$	H-5eq	$\Delta\delta_H$	H-6	$\Delta\delta_H$	H-2′	$\Delta\delta_H$	H-3′$_{proR}$	$\Delta\delta_H$	H-3′$_{proS}$	$\Delta\delta_H$	C-1′ config
S	1.60		2.19		4.46		1.57		0.80		1.10		
		+0.12		+0.19		+0.09		−0.11		−0.10		−0.03	*S*
R	1.48		2.00		4.37		1.68		0.90		1.13		

[a]Data registered in $CDCl_3$ at 300 MHz.

the *R*- and *S*-MTPA esters (Figure S22, Supporting Information) of compound **11** indicated the absolute configuration of C-1′ to be *S*. Therefore, the absolute configuration for C-6, C-1′, C-2′, C-4′, and particularly the previously unassigned C-6′[10,11] was confirmed as 6*R*, 1′*S*, 2′*S*, 4′*S*, and 6′*S* according to the relative configuration obtained from X-ray diffraction analysis of **9** (Figure 2). Additionally, in order to validate that all stereogenic centers at the 6-heptyl-5,6-dihydro-2*H*-pyran-2-one core of brevipolides were identical, saponification of compounds **11** and **12** was conducted, providing the same optically active functionalized dodecanoic acid methyl ester **13**.

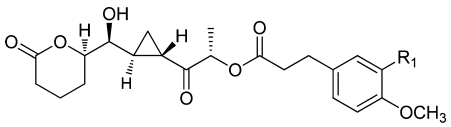

11 R_1 = H
12 R_1 = OH

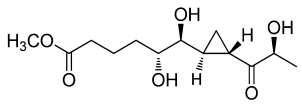

13

Chiroptical measurements of **7**−**10** were undertaken to explore the electronic circular dichroism (ECD) spectra of the brevipolide series. A positive n→π* Cotton effect for the α,β-unsaturated δ-lactone was observed for the four compounds centered at λ_{max} 259−264 nm, confirming that the stereogenic center at C-6 is *R* (Figure S23, Supporting Information), as it has been described in all 6-substituted 5,6-dihydro-α-pyrones from the mint familiy.[4] ECD for the chiral *trans*-cinnamoyl derivatives **7**, **8**, and **10** exhibited a positive Cotton effect centered around 300 nm, in contrast with the *cis*-compound **9**, which showed a negative Cotton effect at 319 nm ($\Delta\varepsilon$ = −1.3). It is important to note that this effect was not previously reported[10,11] because of the fact that brevipolides were isolated as mixtures in different degrees of both geometric isomers where the positive Cotton effect for the *trans*-isomer overlapped the negative one for the *cis*-compound.

A molecular model for compound **9** was generated to correlate the 3D structure with its spectroscopic and chiroptical properties. The starting geometry was modeled by taking into account the configuration and conformation of the 6-heptyl-5,6-dihydro-2*H*-pyran-2-one framework from the X-ray diffraction data (Figure 2). A systematic search afforded 108 conformers even though several conformational arrangements were discarded because of the presence of hindering steric effects, partial atomic overlapping, or a high MMFF[16] energy. The 64 contributing conformers were geometrically optimized at the B3LYP/DGDZVP level.[17] Table S2 lists the relative free energies as well as the Boltzmann distribution for the most relevant conformers within a ΔG° range of between 0 and 3.3 kcal mol^{-1}, offering evidence for the flexibility of this molecule.[12,13] The magnetic shielding tensors were calculated with the gauge-including atomic orbital method, followed by theoretical calculation of the NMR spin−spin coupling constants at the B3LYP/DGDZVP level. These values were Boltzmann-averaged to yield DFT-calculated coupling constants according to protocols previously described.[12,13] The theoretical values showed good correlation with the experimentally registered J_{H-H} for **9** (Table 3), reflecting the conformational behavior of the brevipolide core in solution. The solid-state conformation (Figure 2) is different from all the minimum energy conformers (Figure 3), perhaps as a result of the replacement of the intermolecular hydrogen bonding (Figure S24, Supporting Information) with a $C_1-O_1\cdots H-O_{1'}-C_{1'}$ intramolecular bond. The release of the crystal-packing constraints promotes the presence of multiple conformational arrangements that fulfill the entropic requirements for this flexible system as predicted by DFT modeling (Table 3). Also, the most relevant conformers **9a**−**9f**, accounting for 88% of the conformational population, were useful to rationalize the observed NOESY correlations as shown in Figure 3. The global minimum **9a** is responsible for the observed correlations between $H_6-H_{1'}$, $H_{1'}-H_{3'proR}$, and $H_{4'}-H_{6'}$, while the second minimum **9b** produces the complementary interactions between $H_{5eq}-H_{2'}$ and $H_{1'}-H_{4'}$. The subsequent conformers also contribute to enhance the above-mentioned effects. The NMR features are consistent along the brevipolide series, indicating that the conformational behavior in solution for the 6-heptyl-5,6-dihydro-2*H*-pyran-2-one core in compounds **1**−**10** is essentially the same, e.g., $^3J_{HH}$ (Table S1, Supporting Information) and observed NOEs for the new compound **10** (Figure S15, Supporting Information).

The molecular models for the most stable conformers of **9** (Figure 3) were also useful to provide validation for the observed lowest energy negative Cotton effect in the ECD spectra of *cis*-isomer **9**. TDDFT calculations[18] were carried out to corroborate the sign for the n→π* transition corresponding to the chirally substituted 4-methoxy-*cis*-cinnamoyl moiety.[19] Negative values for the main conformers **9a**−**9f** were obtained ranging from λ = 316 to 324 nm with $R_{velocity}$ between −1.3 and −136.9 × 10^{-40} erg·esu·cm·Gauss^{-1} (Table 4), in agreement with the experimental value (Figure S23, Supporting Information). Additionally, the same theoretical protocol was applied to calculate the n→π* transitions for the hypothetical $C_{6'}$-(*R*)-epimer of brevipolide I. The main conformers of this structure (**$C_{6'}$*R*-9a** to **$C_{6'}$*R*-9a**) showed positive values for the lowest energy transition, within the range from λ = 313 to 328 nm with $R_{velocity}$ between 42.3 and 128.1 × 10^{-40} erg·esu·cm·Gauss^{-1} (Table 4).

In conclusion, the present investigation exemplified a protocol for stereochemical analysis by application of a combined theoretical and experimental methodology.[13] The absolute configuration and conformation of the brevipolide

dx.doi.org/10.1021/np300740h | J. Nat. Prod. 2013, 76, 72−78

Table 3. DFT B3LYP/DGDZVP Relative Free Energies,[a] Population,[b] and Comparison between DFT and Experimental $^1H-^1H$ Coupling Constants[c] for the 20 Lowest Energy Conformers of Brevipolide I (9)

conformer	ΔG^a	P^b	J_{3-4}	J_{4-5eq}	J_{4-5ax}	J_{5eq-6}	J_{5ax-6}	$J_{6-1'}$	$J_{1'-2'}$	$J_{2'-3'proS}$	$J_{2'-3'proR}$	$J_{2'-4'}$	$J_{3'proS-4'}$	$J_{3'proR-4'}$
9a	0.000	28.2	9.75	7.16	2.41	3.94	12.82	2.54	1.20	9.70	6.26	3.19	3.92	8.23
9b	0.100	23.8	9.81	6.95	2.34	3.98	12.62	2.74	10.38	9.02	6.61	2.91	3.99	8.81
9c	0.307	16.8	9.74	7.14	2.42	4.00	12.81	2.47	10.27	9.71	6.07	3.19	3.93	8.20
9d	0.671	9.1	9.80	6.85	2.27	3.67	12.35	8.65	9.36	9.68	6.08	2.68	4.71	7.67
9e	1.029	5.0	9.81	6.73	2.31	3.56	13.65	8.04	1.12	8.88	6.28	3.23	3.55	8.73
9f	1.060	4.7	9.79	6.97	2.36	4.01	12.72	2.63	9.24	9.59	6.02	3.81	3.43	9.77
9g	1.349	2.9	9.79	6.97	2.36	4.01	12.72	2.66	8.99	9.59	6.04	3.86	3.43	9.87
9h	1.474	2.3	9.79	6.83	2.26	3.69	12.36	8.60	9.55	9.54	5.74	3.10	3.66	9.41
9i	1.669	1.7	9.73	6.71	2.29	3.55	14.05	2.45	9.81	8.99	5.54	3.17	5.21	7.34
9j	1.682	1.6	9.81	6.96	2.35	3.97	12.61	2.63	10.53	8.98	5.52	2.70	3.87	8.12
9k	2.184	0.7	9.82	6.82	2.30	3.39	13.75	2.94	1.63	9.51	5.90	3.94	3.58	9.57
9l	2.334	0.5	9.80	6.81	2.26	3.82	12.38	8.78	2.19	9.53	6.21	3.75	3.96	8.90
9m	2.391	0.5	9.78	6.88	2.36	3.90	12.73	1.44	10.81	9.10	5.84	3.06	3.46	9.15
9n	2.397	0.5	9.80	6.81	2.26	3.83	12.38	8.76	2.20	9.54	6.22	3.74	3.98	8.87
9o	2.566	0.4	9.80	6.82	2.26	3.78	12.40	8.74	2.35	9.52	6.18	3.66	4.13	8.70
9p	2.610	0.3	9.81	6.82	2.27	3.82	12.39	8.75	2.40	9.50	6.17	3.68	4.10	8.73
9q	2.679	0.3	9.82	6.79	2.30	3.46	13.78	2.89	1.52	9.51	5.90	3.86	3.60	9.49
9r	2.698	0.3	9.81	6.81	2.26	3.88	12.39	8.77	2.02	9.56	6.23	3.70	3.97	8.86
9s	2.905	0.2	9.82	7.00	2.45	3.16	13.87	3.89	2.90	9.55	5.60	3.25	4.46	7.76
9t	3.545	0.1	9.73	6.92	2.30	3.59	12.96	1.21	11.18	9.12	5.18	3.34	3.80	9.44
	weighted values[c,d]		9.78	7.01	2.36	3.90	12.77	3.68	6.83	9.45	6.23	3.13	3.97	8.50
	experimental values[e]		9.70	6.50	2.20	3.80	12.30	3.80	6.30	8.90	6.00	3.40	3.90	8.10

[a]In kcal/mol. [b]In percent from $\Delta G°$ values at 298 K and 1 atm, $G_{global} = -1379.11433$ kcal/mol. [c]In Hz calculated from the B3LYP/DGDZVP structures. [d]$\sum_i J_i \times P_i$, where J_i is the coupling constant value for each conformer and P_i is the population for the ith conformation. [e]Couplings obtained by spectral simulation.

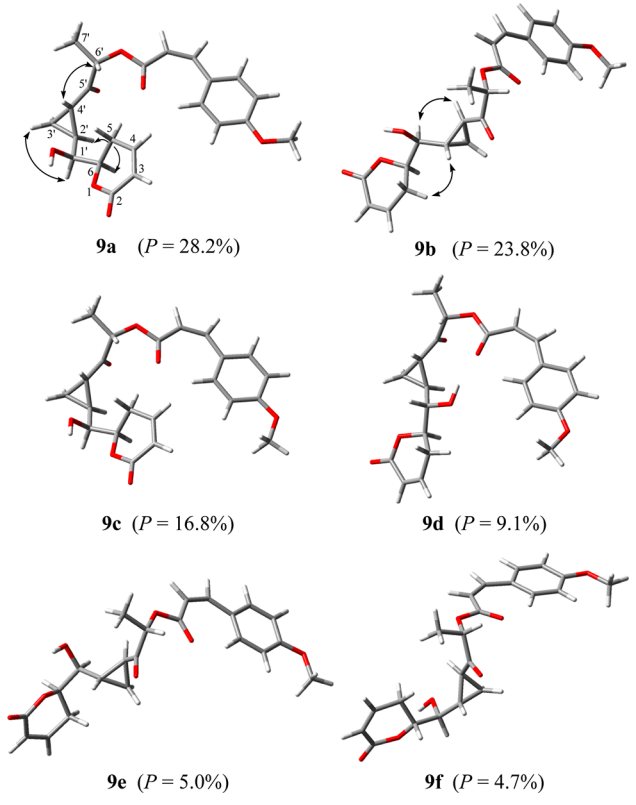

Figure 3. The most relevant conformers of brevipolide I (**9**) accounting for 88% of the conformational population. NOESY correlations are indicated with arrows in the global minimum (**9a**) and the second lowest energy minimum (**9b**).

Table 4. Calculated Energy, Wavelength, and Oscillator and Rotatory Strengths for the Lowest Energy n→π* Transition of Brevipolide I (9) and Its Hypothetical $C_{6'}$-(*R*)-Epimer at the B3LYP/DGDZVP Level of Theory

conformer $(P)^a$	ΔE^b	$\lambda_{max}{}^c$	f^d	$R_{velocity}{}^e$	$R_{length}{}^f$
9a (28.2)	3.929	316	0.662	−1.26	−2.30
9b (23.8)	3.899	318	0.661	−136.87	−134.59
9c (16.8)	3.886	319	0.572	−4.55	−4.03
9d (9.1)	3.827	324	0.565	−88.65	−89.75
9e (5.0)	3.906	317	0.660	−108.73	−107.05
9f (4.7)	3.896	318	0.670	−127.95	−126.58
$C_{6'}$*R*-**9a** (39.2)	3.915	317	0.692	82.15	79.61
$C_{6'}$*R*-**9b** (29.5)	3.774	328	0.577	128.06	127.54
$C_{6'}$*R*-**9c** (11.5)	3.942	315	0.667	60.00	57.20
$C_{6'}$*R*-**9d** (8.0)	3.859	321	0.573	123.14	119.62
$C_{6'}$*R*-**9e** (3.6)	3.920	316	0.696	55.14	55.82
$C_{6'}$*R*-**9f** (2.7)	3.966	313	0.748	42.27	42.77

[a]Conformational population in percentage is given in parentheses. [b]Excitation energy in eV. [c]Wavelength in nm. [d]Oscillator strength. [e]Rotatory strength in velocity form ($\times 10^{-40}$ erg·esu·cm·Gauss^{-1}). [f]Rotatory strength in length form ($\times 10^{-40}$ erg·esu·cm·Gauss^{-1}).

series were established by the systematic comparison between theoretical and experimental vicinal ^1H NMR coupling constants and DFT ECD calculations. These results provided support for the (6′*S*)-configuration in this class of bioactive compounds from the mint family.

EXPERIMENTAL SECTION

General Experimental Procedures. Melting points were determined on a Fisher-Johns apparatus and are uncorrected. Optical

dx.doi.org/10.1021/np300740h | J. Nat. Prod. 2013, 76, 72−78

rotations were measured with a Perkin-Elmer model 341 polarimeter. ^{1}H (400 and 300 MHz) and ^{13}C (100 and 75 MHz) NMR experiments were registered on a Varian Inova instrument. Positive-ion HRFABMS were recorded using a matrix of 3-nitrobenzyl alcohol on a Thermo DFS spectrometer. Analytical and semipreparative HPLC analysis were carried out on Waters equipment (Millipore Corp., Waters Chromatography Division, Milford, MA, USA), which was composed of a 600E multisolvent delivery system equipped with a 996 photodiode array detector. Empower 2 software was used to control equipment and for data acquisition, processing, and management of the chromatographic information.

Plant Material. Aerial parts of *Hyptis brevipes* were collected in Dos Ríos, Municipio de Emiliano Zapata, Veracruz, Mexico, in November 2009. The plant material was identified by A.H.-R., and a voucher specimen has been deposited in the herbarium of the Instituto de Ecología, Xalapa, Veracruz, Mexico (accession number XAL0000247). Also, a voucher specimen was archived at the Botanical Collection of Facultad de Ciencias, Universidad Nacional Autónoma de México (voucher 127321).

Extraction and Isolation. Aerial parts (2 kg) were powdered and extracted exhaustively by maceration at room temperature with $CHCl_3$ to afford, after removal of the solvent, a dark brown syrup (50 g). The extract (50 g) was fractionated by open column chromatography over silica gel (1 kg), using a gradient of hexanes−CH_2Cl_2, followed by CH_2Cl_2−acetone and acetone−MeOH in several proportions. Altogether, 100 eluates (300 mL each one) were collected and combined in 20 fractions. Fraction 12 (2.3 g, eluted with CH_2Cl_2−acetone, 4:1) was fractionated by passage on silica gel (230−400 mesh) and using a gradient of increasing polarity of hexanes−EtOAc, EtOAc−acetone, and acetone−MeOH. A total of 10 pooled subfractions were collected. Subfraction VII (200 mg, eluted with EtOAc−acetone, 9:1) was resolved by HPLC on a Symmetry C_{18} column (Waters; 7 μm, 19 × 300 mm) with an isocratic elution of MeCN−H_2O (2:3) and a flow rate of 7.5 mL/min (sample injection, 500 μL; concentration, 0.1 mg/μL). Eluates across the peaks with t_R values of 37.60 min (peak I) and 40.37 min (peak II) were collected by the technique of heart cutting and independently reinjected in the apparatus operating in the recycle mode to achieve total homogeneity after 5−10 consecutive cycles and employing the same reversed-phase column and the instrumental conditions as described above. These techniques afforded pure compounds **8** (30 mg) from peak I and **9** (15 mg) from peak II. Compound **9** was recrystallized from hexanes−CH_2Cl_2 (4:1).

Fraction 15 (9.0 g, eluted with CH_2Cl_2−acetone, 7:3) was submitted to column chromatography on silica gel (230−400 mesh) using a gradient of increasing polarity of hexanes−EtOAc, EtOAc−acetone, and acetone−MeOH. In total, eigth pooled subfractions were collected. Subfraction VI (100 mg, eluted with EtOAc−acetone) was resolved by HPLC on a Symmetry C_{18} column (Waters; 7 μm, 19 × 300 mm) with an isocratic elution of MeCN−H_2O (7:3) and a flow rate of 9.0 mL/min (sample injection, 500 μL; concentration, 0.1 mg/μL). Eluates across the peaks with t_R values of 31.04 min (peak III) and 34.79 min (peak IV) were collected by the technique of heart cutting and independently reinjected (sample injection, 500 μL; concentration, 0.1 mg/μL) in the apparatus operating in the recycle mode to achieve total homogeneity after 10 cycles. These techniques afforded pure compound **7** (15 mg) from peak III and compound **10** (12 mg) from peak IV.

*Brevipolide G (**7**):* colorless oil; ORD (*c* 0.08, $CHCl_3$) $[\alpha]_{589}$ +138.7, $[\alpha]_{578}$ +142.5, $[\alpha]_{546}$ +167.5, $[\alpha]_{436}$ +361.2; ECD (*c* 5.5 × 10^{-5} M, MeCN) λ_{max} ($\Delta\varepsilon$) 230 (−2.99), 260 (+4.22), 301 (+4.02); ^{1}H NMR (300 MHz, $CDCl_3$) and ^{13}C NMR (75 MHz, $CDCl_3$) data (Figures S3 and S4, Supporting Information), see Table S1 (Supporting Information); HRFABMS *m*/*z* 387.1455 $[M + H]^+$ (calcd for $C_{22}H_{23}O_7$, 387.1438).

*Brevipolide H (**8**):* colorless solid; mp 114−116 °C; ORD (*c* 0.24, $CHCl_3$) $[\alpha]_{589}$ +157.5, $[\alpha]_{578}$ +165, $[\alpha]_{546}$ +195, $[\alpha]_{436}$ +421, $[\alpha]_{365}$ +1067.9; ECD (*c* 2.8 × 10^{-5} M, MeCN) λ_{max} ($\Delta\varepsilon$) 230 (−3.71), 259 (+3.83), 305 (+8.54); ^{1}H NMR (400 MHz, $CDCl_3$) and ^{13}C NMR (100 MHz,$CDCl_3$) data (Figures S5 and S6, Supporting Information), see Table S1 (Supporting Information); HRFABMS *m*/*z* 401.1595 $[M + H]^+$ (calcd for $C_{22}H_{25}O_7$, 401.1522).

*Brevipolide I (**9**):* colorless prisms; mp 124−125 °C; ORD (*c* 0.15, $CHCl_3$) $[\alpha]_{589}$ +36,$[\alpha]_{578}$ +37.3, $[\alpha]_{546}$ +42, $[\alpha]_{436}$ +59; ECD (*c* 2.2 × 10^{-5} M, MeCN) λ_{max} ($\Delta\varepsilon$) 229 (−0.91), 264 (+2.20), 319 (−1.26); ^{1}H NMR (300 MHz, $CDCl_3$) and ^{13}C NMR (75 MHz,$CDCl_3$) data (Figures S7 and S8, Supporting Information), see Table S1 (Supporting Information); HRFABMS *m*/*z* 401.1595 $[M + H]^+$ (calcd for $C_{22}H_{25}O_7$, 401.1522).

*Brevipolide J. (**10**):* colorless oil; ORD (*c* 0.17, $CHCl_3$) $[\alpha]_{589}$ +147.0, $[\alpha]_{578}$ +156.5, $[\alpha]_{546}$ +183.5, $[\alpha]_{436}$ +392.9; ECD (*c* 8.6 × 10^{-5} M, MeCN) λ_{max} ($\Delta\varepsilon$) 229 (−4.11), 262 (+6.11), 294 (+5.83); ^{1}H NMR (300 MHz, $CDCl_3$) and ^{13}C NMR (75 MHz,$CDCl_3$) data, see Table 1 (Figures S9 and S10, Supporting Information); HRFABMS *m*/*z* 416.1467 $[M + H]^+$ (calcd for $C_{22}H_{25}O_7$, 416.1471).

Methylation of Compound 7. A MeOH solution of **7** (3 mg/100 μL) was treated with CH_2N_2 in Et_2O (1 mL) at 0 °C. The solution was monitored over 1 h by TLC until reaction completion and dissipation of the yellow color. The solvent was evaporated under reduced pressure inside a fume-hood to afford a product that was identical to compound **8** (3 mg).

Hydrogenation of Compounds 8−10. A solution of compounds **8** and **9** (15 mg each) in THF was treated with Pd/C (5% mol, 0.045g) under a N_2 atmosphere during 15 min. The solution was transferred to a 45 mL stainless steel Parr reactor and pressurized with H_2 (200 psi) at room temperature during 24 h.[20] Then, the excess of gas was released. The residue was filtered, concentrated under vacuum, and purified by HPLC on a Symmetry C_{18} column (Waters; 7 μm, 19 × 300 mm) with an isocratic elution of MeCN−H_2O and a flow rate of 9.0 mL/min (sample injection, 500 μL; concentration, 0.06 mg/μL). These procedures afforded pure compound **11** (25 mg) as the only reaction product. The same process was individually applied to each pure natural product **8** and **9** (3 mg) to afford a convergent derivative (2.5 mg) that was chromatographically (HLPC coelution experiments, t_R 30.68 min) and spectroscopically (NMR) identical with compound **11**. Compound **10** (5 mg) was also subjected to the same hydrogenation protocol to generate the tetrahydro derivative **12**.

*Tetrahydro derivative **11**:* colorless oil; ORD (*c* 0.36, $CHCl_3$) $[\alpha]_{589}$ +46.4, $[\alpha]_{578}$ +48.3, $[\alpha]_{546}$ +56.7, $[\alpha]_{436}$ +115.8, $[\alpha]_{365}$ +242.8; ^{1}H NMR (300 MHz, $CDC1_3$) δ 7.11 (d, *J* = 8.7 Hz, H-2″ and H-6″), 6.82 (d, *J* = 8.7 Hz, H-3″ and H-5″), 5.16 (q, *J* = 7.1 Hz, H-6′), 4.39 (ddd, *J* = 10.8, 3.2, 3.2 Hz, H-6), 3.78 (s, OCH_3), 3.54 (dd, *J* = 6.1, 3.2 Hz, H-1′), 2.90 (t, *J* = 7.4 Hz, H-8″), 2.68 (t, *J* = 7.4 Hz, H-7″), 2.67 (m, H-3ax), 2.47 (m, H-3eq), 2.10 (ddd, *J* = 8.5, 3.9, 3.4 Hz, H-4′), 1.98−1.75 (4m, H-4ax, H-4eq, H-5ax, and H-5eq), 1.54 (dddd, *J* = 8.9, 6.3, 6.3, 3.4 Hz, H-2′), 1.43 (d, *J* = 7.1 Hz, Me-7′), 1.27 (ddd, *J* = 8.5, 4.0, 3.9 Hz, H-3′$_{proS}$), 1.02 (ddd, *J* = 8.9, 6.3, 4.0 Hz, H-3′$_{proR}$) (Figure S16, Supporting Information); ^{13}C NMR (75 MHz, $CDC1_3$) δ 206.5 (C-5′), 173.1 (C-9″), 171.7 (C-2), 158.1 (C-4″), 132.3 (C-1″), 129.3 (C-2″ and C-6″), 113.9 (C-3″ and C-5″), 83.3 (C-6), 75.2 (C-6′), 72.5 (C-1′), 55.3 (OCH_3), 35.8 (C-8″), 29.9 (C-7″), 29.8 (C-3), 26.4 (C-2′), 21.6 (C-5), 21.3(C-4′), 18.4 (C-4), 15.6 (C-7′), 14.3 (C-3′) (Figure S17, Supporting Information); HRFABMS *m*/*z* 405.1875 $[M + H]^+$ (calcd for $C_{22}H_{29}O_7$, 405.1908).

*Tetrahydro Derivative **12**:* colorless oil; ORD (*c* 0.12, $CHCl_3$) $[\alpha]_{589}$ +39.2, $[\alpha]_{578}$ +40.0, $[\alpha]_{546}$ +46.7, $[\alpha]_{436}$ +95.0, $[\alpha]_{365}$ +190.8; ^{1}H NMR (300 MHz, $CDC1_3$) δ 7.06 (d, *J* = 1.9 Hz, H-2″), 6.80 (d, *J* = 8.2 Hz, H-5″), 6.71 (dd, *J* = 8.2, 1.9 Hz, H-6″), 5.20 (q, *J* = 7.1 Hz, H-6′), 4.42 (ddd, *J* = 10.7, 3.1, 3.1 Hz, H-6), 3.89 (s, OCH_3), 3.54 (dd, *J* = 6.3, 3.3 Hz, H-1′), 2.90 (t, *J* = 7.1 Hz, H-8″), 2.71 (t, *J* = 7.1 Hz, H-7″), 2.70−2.45 (2m, H-3ax and H-3eq), 2.13 (ddd, *J* = 8.5, 3.9, 3.4 Hz, H-4′), 2.10−1.80 (4m, H-4ax, H-4eq, H-5ax, and H-5eq), 1.57 (dddd, *J* = 8.9, 6.3, 6.3, 3.4 Hz, H-2′), 1.47 (d, *J* = 7.1 Hz, H-7′), 1.32 (ddd, *J* = 8.5, 4.0, 3.9 H-3′$_{proS}$), 1.04 (ddd, *J* = 8.9, 6.3, 4.0 Hz, H-3′$_{proR}$) (Figure S18, Supporting Information); ^{13}C NMR (75 MHz, $CDC1_3$) δ 206.6 (C-5′), 172.5 (C-9″), 171.5 (C-2), 145.5 (C-3″) 145.1 (C-4″), 133.6 (C-1″), 119.7 (C-6″), 114.6 (C-2″), 110.8 (C-5″), 83.2 (C-6), 75.3 (C-6′), 72.6 (C-1′), 56.0 (OCH_3), 35.6 (C-8″), 30.1 (C-7″), 29.8 (C-3), 26.5 (C-2′), 21.6 (C-5), 21.3 (C-4′), 18.4 (C-4), 15.9 (C-7′),

dx.doi.org/10.1021/np300740h | *J. Nat. Prod.* 2013, 76, 72−78

14.3 (C-3′) (Figure S19, Supporting Information); HRFABMS *m/z* 420.1779 $[M]^+$ (calcd for $C_{22}H_{28}O_8$, 420.1784).

Preparation of *R*- and *S*-MTPA Ester Derivatives of 11. A solution of compound **11** (3.0 mg) in $CDCl_3$ (0.75 mL) was transferred into a clean NMR tube containing DMPA (0.5 mg) in pyridine-d_5 (0.10 mL). (*S*)- or (*R*)-α-Methoxy-α-(trifluoromethyl)-phenylacetyl chloride (*S*- or *R*-MTPA-Cl) (10 μL) was immediately added into the NMR tube under a N_2 stream.[21] The ^{1}H NMR spectrum of the reaction mixture for each derivative (*S*- or *R*-MTPA-ester) was obtained directly from the reaction tube, which was permitted to stand at room temperature and monitored every 1 h. The reaction was found to be completed after 4 h.

R-MTPA ester of 11: ^{1}H NMR δ 7.03 (d, *J* = 8.6 Hz, H-2″ and H-6″), 6.73 (d, *J* = 8.6 Hz, H-3″ and H-5″), 5.00 (q, *J* = 7.1, H-6′), 4.70 (dd, *J* = 9.5, 2.9 Hz, H-1′), 4.37 (ddd, *J* = 11.0, 3.2, 3.2 Hz, H-6), 2.80 (t, *J* = 7.4 Hz, H-8″), 2.58 (m, H-3ax), 2.55 (t, *J* = 7.4 Hz, H-7″), 2.37 (ddd, *J* = 14.0, 4.0, 4.0 Hz, H-3eq), 2.18 (ddd, *J* = 8.5, 3.9, 3.4 Hz, H-4′), 2.00 (ddd, *J* = 14.0, 10.0, 6.0 Hz, H-5eq), 1.83−1.60 (2m, H-4ax and H-4eq), 1.68 (m, H-2′), 1.48 (dddd, *J* = 14.0, 12.0, 12.0, 3.0 Hz, H-5ax), 1.25 (d, *J* = 7.1 Hz, Me-7′), 1.13 (ddd, *J* = 8.5, 4.0, 3.9 Hz, H-3′$_{proS}$), 0.90 (ddd, *J* = 8.9, 6.3, 4.0 Hz, H-3′$_{proR}$) (Figure S22, Supporting Information).

S-MTPA ester of 11: ^{1}H NMR δ 7.03 (d, *J* = 8.6 Hz, H-2″ and H-6″), 6.72 (d, *J* = 8.6 Hz, H-3″ and H-5″), 5.00 (q, *J* = 7.1 Hz, H-6′), 4.77 (dd, *J* = 8.8, 2.6 H-1′), 4.46 (ddd, *J* = 11.0, 3.1, 3.1 Hz, H-6), 2.82 (t, *J* = 7.4 Hz, H-8″), 2.62 (m, H-3ax), 2.62 (t, *J* = 7.4 Hz, H-7″), 2.48 (ddd, *J* = 14.0, 4.0, 4.0 Hz, H-3eq), 2.19 (ddd, *J* = 14.0, 10.0, 6.0 Hz, H-5eq), 2.17 (ddd, *J* = 8.5, 3.9, 3.4 Hz, H-4′), 1.90−1.60 (2m, H-4ax and H-4eq), 1.60 (dddd, *J* = 14.0, 12.0, 12.0, 3.0 Hz, H-5ax), 1.57 (m, H-2′), 1.26 (d, *J* = 7.1 Hz, Me-7′), 1.10 (ddd, *J* = 8.5, 4.0, 3.9 Hz, H-3′$_{proS}$), 0.80 (ddd, *J* = 8.9, 6.3, 4.0 Hz, H-3′$_{proR}$) (Figure S22, Supporting Information).

Hydrolysis of Compounds 11 and 12. Compound **11** (21.7 mg) was dissolved in MeOH (400 μL), and NaOMe (3.6 mg) was added. The reaction mixture was stirred at room temperature for 1 h. Saturated aqueous NH_4Cl solution was added, and the mixture was diluted with CH_2Cl_2.[22] The organic layer was dried, filtered, and concentrated under reduced pressure. The residue was purified by HPLC on a Symmetry C_{18} column (Waters; 5 μm, 4.6 × 250 mm) with an isocratic elution of MeOH−MeCN (7:3) and a flow rate of 0.3 mL/min (sample injection, 20 μL; concentration, 0.05 mg/μL) to afford pure compound **13** (6 mg). Derivative **12** was also hydrolyzed, and the reaction residue was purified using the same procedures as described above to yield compound **13**.

Compound 13: colorless oil; ORD (*c* 0.07, $CHCl_3$) $[\alpha]_{589}$ +88.6, $[\alpha]_{578}$ +92.9, $[\alpha]_{546}$ +107.1, $[\alpha]_{436}$ +207.1, $[\alpha]_{365}$ +412.9; ^{1}H NMR (300 MHz, $CDC1_3$) δ 4.49 (q, *J* = 7.0 Hz, H-11), 3.74 (m, H-5), 3.71 (s, OCH_3), 3.24 (dd, *J* = 7.4, 3.5 Hz, H-6), 2.42 (t, *J* = 7.1 Hz, H-2a and H-2b), 2.13 (ddd, *J* = 8.5, 3.9, 3.4 Hz, H-9), 1.87 (m, H-3a), 1.74 (2m, H-3b and H-7), 1.59 (2m, H-4a and H-4b), 1.47 (d, *J* = 7.0 Hz, Me-12), 1.37 (ddd, *J* = 8.5, 4.0, 3.9 H-8$_{proS}$), 1.10 (ddd, *J* = 8.9, 6.3, 4.0 Hz, H-8$_{proR}$) (Figure S20, Supporting Information); ^{13}C NMR (75 MHz, $CDC1_3$) δ 211.9.5 (C-10), 174.4 (C-1), 75.6 (C-6), 73.9 (C-5), 73.1 (C-11), 51.7 (OCH_3), 33.6 (C-2), 31.1 (C-4), 26.9 (C-7), 21.4 (C-9), 21.0 (C-3), 19.8 (C-12), 15.5 (C-8) (Figure S21, Supporting Information); EIMS *m/z* 256 $[M - H_2O]^+$ (1), 230 (4), 197 (11), 179 (19), 151 (21), 132 (28), 131 (44), 100 (55), 99 (100), 97 (32), 95 (16), 87 (29), 83 (27), 71 (46), 55 (48); FABMS *m/z* 297 $[M + Na]^+$.

Single-Crystal X-ray Diffraction Analysis of 9. Single-crystal X-ray diffraction analysis was collected on a Bruker SMART APEX CCD diffractometer with graphite-monochromated Mo Kα radiation (λ = 0.71073 Å). Crystal data for **9** were $C_{22}H_{24}O_7$, *M* = 400.41, monoclinic, space group $P2_1$, *a* = 8.9649(12) Å, *b* = 7.7800(11) Å, *c* = 14.731(2) Å, β = 98.250(2)°, *V* = 1016.9(1) Å^3, *Z* = 2, ρ = 1.31 mg/mm^3, λ(Mo Kα) = 0.71073 Å, total reflections = 7442, independent reflections 2617 (R_{int} 0.04%), final *R* indices [$I > 2\sigma(I)$], R_1 = 4.20%, wR_2 = 5.25%. For the structural refinement, the non-hydrogen atoms were treated anisotropically, and the hydrogen atoms included in the structure factor calculations were refined isotropically. Crystallographic data reported in this paper have been deposited with the Cambridge Crystallographic Data Centre (CCDC 914932). Copies of the data can be obtained free of charge on application to the Director, CCDC, 12 Union Road, Cambridge CB2 1EZ, UK (fax: +44-(0)1223-336033 or e-mail: deposit@ccdc.cam.ac.uk).

Molecular Modeling Calculations. Molecular building and conformational search for isomers **8** and **9** and the corresponding $C_{6'}$-(*R*)-epimer were carried out in the Spartan'04 program[23] using the MMFF94 force-field calculation on a Windows operating system machine. A systematic search protocol was performed in which the torsion angles C(5)−C(6)−C(1′)−C(2′), C(1′)−C(2′)−C(4′)−C(5′), and C(2′)−C(4′)−C(5′)−C(6′) in the side chain were varied by 120°, starting at 60° for each central bond, and the torsion angles of the C(4′)−C(5′)−C(6′)−C(7′) dihedral angles were rotated in steps of 180°. The fragment of cinnamic acid was restricted to its most stable conformation, generating a total of 108 initial conformers for each stereoisomer. The cinnamoyl moiety began at H−C_{sp3}−O−C_{sp2} and C_{sp3}−O−C═O dihedral angles ca. 0°, and conformational explorations for this group were achieved within dihedral angle ranges of +60° and −60°. All structures were minimized to a rmsd gradient of 1×10^{-6} kcal/mol on the potential energy surface. An energy cutoff of 10 kcal/mol was selected in order to have a wide frame of conformers in the Boltzmann distribution. All structures inside the cutoff window were geometrically optimized using the hybrid DFT method B3LYP and basis set DGDZVP (B3LYP/DGDZVP). The optimized structures were used to calculate the thermochemical parameters estimated at 298 K and 1 atm. Magnetic shielding tensors were calculated with the gauge-invariant atomic orbital (GIAO) method. Total NMR spin−spin coupling constants (SSCC, *J* (Hz)) were calculated as the summation of the Fermi contact, diamagnetic spin−orbit, spin-dipolar, and paramagnetic spin−orbit, which were calculated from B3LYP/DGDZVP-optimized structures by using the spin−spin option during the NMR jobs. All quantum mechanical NMR calculations were carried out using the Gaussian 03 program on a Linux operating system in the KanBalam cluster, which includes 1368 AMD Opteron processors at 2.6 GHz and a RAM memory of 3 terabytes. For each job, a maximum of four processors was used and each conformer required four different DFT jobs: geometric optimizations, frequency calculations, SSCC estimations, and TD ECD calculations. The total cpu time consumed in this work was 1.33 × 10^3 h. The free energy equation ($\Delta G = -RT \ln K$) was used to obtain the conformational population, taking into account a cyclic equilibrium at 298 K between the selected conformers of **9** within a 0.0−3.3 kcal/mol window with respect to the global minimum. The free energy values ΔG° were obtained from the vibrational frequency calculations as the sum of electronic and thermal free energies.

Cytotoxicity Assay. Nasopharyngeal (KB), laryngeal (Hep-2), colon (HCT-15), cervix (HeLa), breast (MCF-7),[24] and prostate carcinoma (PC-3) cell lines were maintained in RPMI 1640 medium supplemented with 10% fetal bovine serum and were cultured at 37 °C in an atmosphere of 5% CO_2 in air (100% humidity). The cytotoxicity was determined using the SRB assay.[25] The cells were harvested at log phase of their growth cycle, treated in triplicate with various concentrations of the test samples (0.16−20 μg/mL), and incubated for 72 h at 37 °C as described above. Results are expressed as the concentration that inhibits 50% control growth after the incubation period (IC_{50}). The values were estimated from a semilog plot of the drug concentration (μg/mL) against the percentage of growth inhibition. Vinblastine was included as a positive control drug.

■ ASSOCIATED CONTENT

Ⓢ Supporting Information

^{1}H and ^{13}C NMR spectra of compounds **7**−**13** and DEPTQ-135 and 2D NMR spectra including ^{1}H−^{1}H COSY, HSQC, HMBC, and NOESY of compound **10**. Crystal parameters and X-ray coordinates of **9**. CD spectra for **7**−**10**. Table of cytotoxicity for **7**−**10**. This material is available free of charge via the Internet at http://pubs.acs.org.

AUTHOR INFORMATION

Corresponding Author

*Tel: +52 55 5622-5288. Fax: +52 55 5622 5329. E-mail: pereda@unam.mx.

Notes

The authors declare no competing financial interest.

ACKNOWLEDGMENTS

Financial support was provided by Consejo Nacional de Ciencia y Tecnología (CONACyT, grant 104887). G.A.S.O. is also grateful to CONACyT for a graduate student scholarship (226766). Geometry optimizations and coupling constant calculations were performed in the HP Cluster Platform 4000 (KanBalam) at Departamento de Supercómputo, Dirección General de Servicios de Cómputo Académico, UNAM. Thanks are due to G. Duarte and M. Guzmán (USAI, Facultad de Química, UNAM) for recording of the mass spectra. The authors also acknowledge Dr. A. Toscano for the X-ray crystallographic analysis. We also wish to thank Dr. M. Fragoso-Serrano (Facultad de Química, UNAM) for HPLC assistance and cytotoxicity evaluations.

REFERENCES

(1) Hoffmann, H. M. R.; Rabe, J. *Angew. Chem., Int. Ed. Engl.* **1985**, *24*, 94−110.

(2) (a) Pereda-Miranda, R. In *Phytochemistry of Medicinal Plants*; Arnason, J. T.; Mata, R.; Romeo, J. T., Eds.; Plenum: New York, 1995; pp 83−112. (b) Falomir, E.; Murga, J.; Ruiz, P.; Carda, M.; Marco, J. A.; Pereda-Miranda, R.; Fragoso-Serrano, M.; Cerda-García-Rojas, C. M. *J. Org. Chem.* **2003**, *68*, 5672−5676.

(3) (a) Pereda-Miranda, R.; Hernández, L.; Villavicencio, M. J.; Novelo, M.; Ibarra, P.; Chai, H.; Pezzuto, J. M. *J. Nat. Prod.* **1993**, *56*, 583−593. (b) Fragoso-Serrano, M.; Gibbons, S.; Pereda-Miranda, R. *Planta Med.* **2005**, *71*, 278−280.

(4) (a) Davies-Coleman, M. T.; Rivett, D. E. A. In *Progress in the Chemistry of Organic Natural Products*; Herz, W.; Grisebach, H.; Kirby, G. W.; Tamm, Ch., Eds.; Springer: New York, 1989; Vol. *55*, pp 1−35. (b) Collet, L. A.; Davies-Coleman, M. T. Rivett, D. E. A. In *Progress in the Chemistry of Organic Natural Products*; Herz, W.; Falk, H.; Kirby, G. W.; Moore, R. E.; Tamm, Ch., Eds.; Springer: New York, 1998; Vol. *75*, pp 182−209.

(5) (a) Davies-Coleman, M. T.; Rivett, D. E. A. *Phytochemistry* **1996**, *41*, 1085−1092. (b) Collet, L. A.; Davies-Coleman, M. T; Rivett, D. E. A; Drewes, S. E; Horn, M. M. *Phytochemistry* **1997**, *44*, 935−938.

(6) (a) Collet, L. A.; Davies-Coleman, M. T; Rivett, D. E. A. *Phytochemistry* **1998**, *48*, 651−656. (b) Collet, L. A.; Davies-Coleman, M. T; Rivett, D. E. A. *Phytochemistry* **1995**, *38*, 791−792.

(7) Pereda-Miranda, R.; Fragoso-Serrano, M.; Cerda-García-Rojas, C. M. *Tetrahedron* **2001**, *57*, 47−53.

(8) Boalino, D. M.; Connolly, J. D.; McLean, S.; Reynolds, W. F. *Phytochemistry* **2003**, *64*, 1303−1307.

(9) (a) Usui, T.; Watanabe, H.; Nakayama, H.; Tada, Y.; Kanoh, N.; Kondoh, M.; Asao, T.; Takio, K.; Watanabe, H.; Nishikawa, K.; Kitahara, T.; Osada, H. *Chem. Biol.* **2004**, *11*, 799−806. (b) Yoshida, M.; Matsui, Y.; Ikarashi, Y.; Usui, T.; Osada, H.; Wakasugi, H. *Anticancer Res.* **2007**, *27*, 729−736. (c) Vogt, A.; McPherson, P. A.; Shen, X.; Balachandran, R.; Zhu, G.; Raccor, B. S.; Nelson, S. G.; Tsang, M.; Day, B. W. *Chem. Biol. Drug Des.* **2009**, *74*, 358−368.

(10) Deng, Y.; Balunas, M. J.; Kim, J.-A.; Lantvit, D. D.; Chin, Y.-W.; Chai, H.; Sugiarso, S.; Kardono, L. B. S.; Fong, H. H. S.; Pezzuto, J. M.; Swanson, S. M.; Carcache-Blanco, E. J.; Kinghorn, A. D. *J. Nat. Prod.* **2009**, *72*, 1165−1169.

(11) Hegde, V. R.; Pu, H.; Patel, M.; Das, P. R.; Strizki, J.; Gullo, V. P.; Chou, C.-C.; Buevich, A. V.; Chan, T.-M. *Bioorg. Med. Chem. Lett.* **2004**, *14*, 5339−5342.

(12) Mendoza-Espinoza, J. A.; López-Vallejo, F.; Fragoso-Serrano, M.; Pereda-Miranda, R.; Cerda-García-Rojas, C. M. *J. Nat. Prod.* **2009**, *72*, 700−708.

(13) López-Vallejo, F.; Fragoso-Serrano, M.; Suárez-Ortiz, G. A.; Hernández-Rojas, A. C.; Cerda-García-Rojas, C. M.; Pereda-Miranda, R. *J. Org. Chem.* **2011**, *76*, 6057−6066.

(14) Pereda-Miranda, R.; Hérnandez-Carlos, B. *Tetrahedron* **2002**, *58*, 3145−3154.

(15) (a) Kusumi, T.; Hamada, T.; Ishitsuka, M. O.; Othani, T.; Kakisawa, H. *J. Org. Chem.* **1992**, *57*, 1033−1035. (b) Seco, J. M.; Quiñoá, E.; Riguera, R. *Chem. Rev.* **2004**, *104*, 17−117.

(16) (a) Halgren, T. *J. Comput. Chem.* **1996**, *17*, 490−519. (b) Halgren, T. *J. Comput. Chem.* **1996**, *17*, 520−552. (c) Halgren, T. *J. Comput. Chem.* **1996**, *17*, 553−586. (d) Halgren, T.; Nachbar, R. B. *J. Comput. Chem.* **1996**, *17*, 587−615. (e) Halgren, T. *J. Comput. Chem.* **1996**, *17*, 616−641.

(17) (a) Godbout, N.; Salahub, D. R.; Andzelm, J.; Wimmer, E. *Can. J. Chem.* **1992**, *70*, 560−571. (b) Andzelm, J.; Wimmer, E. *J. Chem. Phys.* **1992**, *96*, 1280−1303.

(18) (a) Cerda-García-Rojas, C. M.; García-Gutiérrez, H. A.; Hernández-Hernández, J. D.; Román-Marín, L. U.; Joseph-Nathan, P. *J. Nat. Prod.* **2007**, *70*, 1167−1172. (b) Ding, Y.; Li, X.-C.; Ferreira, D. *J. Nat. Prod.* **2009**, *72*, 327−335.

(19) Choudhary, M. I.; Naheed, N.; Abbaskhan, A.; Ali, S.; Atta-ur-Rahman.. *Phytochemistry* **2009**, *70*, 1467−1473.

(20) Tolmacheva, N. A.; Gerus, I. I.; Dolovanyuk, V. G.; Kondratov, I. S.; Haufe, G. *Eur. J. Org. Chem.* **2009**, *29*, 5012−5019.

(21) (a) Rieser, M. J.; Hui, Y. H.; Rupprecht, J. K.; Kozlowski, J. F.; Wood, K. V.; McLaughlin, J. L.; Hanson, P. R.; Zhuang, Z.; Hoye, T. R. *J. Am. Chem. Soc.* **1994**, *114*, 10203−10213. (b) Fragoso-Serrano, M.; González-Chimeo, E.; Pereda-Miranda, R. *J. Nat. Prod.* **1999**, *62*, 45−50.

(22) O'Malley, S. J.; Tan, K. L.; Watzke, A.; Bergman, R. G.; Ellman, J. A. *J. Am. Chem. Soc.* **2005**, *127*, 13496−13497.

(23) Kong, J.; White, C. A.; Krylov, A. I.; Sherrill, C. D.; Adamson, R. D.; Furlani, T. R.; Lee, M. S.; Lee, A. M.; Gwaltney, S. R.; Adams, T. R.; Ochsenfeld, C.; Gilbert, A. T. B.; Kedziora, G. S.; Rassolov, V. A.; Maurice, D. R.; Nair, N.; Shao, Y.; Besley, N. A.; Maslen, P. E.; Dombroski, J. P.; Daschel, H.; Zhang, W.; Korambath, P. P.; Baker, J.; Byrd, E. F. C.; Van Voorhis, T.; Oumi, M.; Hirata, S.; Hsu, C.-P.; Ishikawa, N.; Florian, J.; Warshel, A.; Johnson, B. G.; Gill, P. M. W.; Head-Gordon, M.; Pople, J. A. *J. Comput. Chem.* **2000**, *21*, 1532−1548.

(24) Figueroa-González, G.; Jacobo-Herrera, N.; Zentella-Dehesa, A.; Pereda-Miranda, R. *J. Nat. Prod.* **2012**, *75*, 93−97.

(25) (a) Skehan, P.; Storeng, R.; Scudiero, D.; Monks, A.; McMahon, J.; Vistica, D.; Warren, J. T.; Bokesch, H.; Kenney, S.; Boyd, M. R. *J. Natl. Cancer Inst.* **1990**, *82*, 1107−1112. (b) Vichai, V.; Kirtikara, K. *Nat. Protoc.* **2006**, *1*, 1112−1116.